

Electromagnetic shielding effectiveness and mechanical properties of graphite-based polymeric films

G. Kenanakis¹ · K. C. Vasilopoulos¹ · Z. Viskadourakis² · N.-M. Barkoula³ · S. H. Anastasiadis^{1,4} · M. Kafesaki^{1,5} · E. N. Economou¹ · C. M. Soukoulis^{1,6}

Received: 26 May 2016 / Accepted: 2 August 2016
© Springer-Verlag Berlin Heidelberg 2016

Abstract Modern electronics have nowadays evolved to offer highly sophisticated devices. It is not rare; however, their operation can be affected or even hindered by the surrounding electromagnetic radiation. In order to provide protection from undesired external electromagnetic sources and to ensure their unaffected performance, electromagnetic shielding is thus necessary. In this work, both the electromagnetic and mechanical properties of graphite-based polymeric films are studied. The investigated films show efficient electromagnetic shielding performance along with good mechanical stiffness for a certain graphite concentration. To the best of our knowledge, the present study illustrates for the first time both the electromagnetic shielding and mechanical properties of the polymer composite samples containing graphite filler at such high concentrations (namely 60–70 %). Our findings indicate that

these materials can serve as potential candidates for several electronics applications.

1 Introduction

A typical problem in high-frequency electronic devices, such as cell phones and laptops, aircraft electronics and medical devices, is that their performance is influenced by the existence of neighbor electronic instruments. This “electromagnetic interference” (EMI) can cause malfunction of sensitive devices, primarily medical equipment, and as a result, they can become unsafe or, even, harmful to life. Thus, the control of both the incoming and the outgoing EMI level of an electronic device is essential, in order to maintain its functionality and integrity [1–4].

In order to eliminate the EMI effects, it is necessary to develop materials that can either absorb or reflect the electromagnetic radiation of a particular range of frequencies, offering this way electromagnetic shielding [1, 2]. Several EMI shielding materials have been proposed, such as metallic cabinets and conductive coatings or polymers, to name but a few [2, 3]. Metal-based shielding materials, although they are the most widely used EMI protectors, suffer from several drawbacks, such as their heavy weight (especially in applications where mass should be as low as possible), their sensitivity to corrosion, their lack of flexibility and their expensive processing [1–3]. As a result, during the last years, the scientific community has been working on the direction of new EMI shielding materials, like conducting nanostructured layers and composites, which have been gaining popularity for electromagnetic shielding applications, especially in the GHz frequency range [4–7]. For example, polymer composites containing carbon-based fillers (e.g., graphite, carbon black, carbon

✉ G. Kenanakis
gkenanak@iesl.forth.gr

¹ Institute of Electronic Structure and Laser, Foundation for Research & Technology-Hellas, N. Plastira 100, 70013 Heraklion, Crete, Greece

² Crete Center for Quantum Complexity and Nanotechnology, University of Crete, 71003 Heraklion, Greece

³ Department of Materials Engineering, University of Ioannina, 45110 Ioannina, Greece

⁴ Department of Chemistry, University of Crete, 71003 Heraklion, Crete, Greece

⁵ Department of Materials Science and Technology, University of Crete, 71003 Heraklion, Crete, Greece

⁶ Ames Laboratory, U.S. Department of Energy and Department of Physics and Astronomy, Iowa State University, Ames, IA 50011, USA

fibers and/or carbon nanofibers [4–10]) have been investigated as shielding materials, due to their unique combination of electrical conduction, polymeric flexibility and light-weight. More recently, the EMI capabilities of shielding materials based on polyaniline and graphene, carbon nanotubes or carbon nanofibers have been investigated [4, 7, 11, 12], since these carbon nanofillers exhibit lower percolation thresholds and superior electrical properties. However, the applications of such conductive additives are limited due to their high processing costs [13].

Several works have been reported regarding conductive polymer composite materials based on polyethylene or polypropylene with sufficient EMI shielding properties [5, 14–16]. On the other hand, among various polymers, thermoplastic polystyrene offers certain advantages for numerous applications, such as its high glass transition temperature allowing its use as a structural material over an extended temperature range or the possibility to be recycled into domestic building products, whereas it offers quite significant soundproofing and thermal insulation properties. Moreover, it exhibits high resistance to shrinkage, maintaining its strength and shape for long periods of time. Finally, it is worth mentioning that since its many applications include building, roof and piping insulation, display cases for appliances, packaging and laboratory equipment, its combination with conductive (nano)additives can produce composites that can offer adequate EMI shielding properties with many potential applications indoors and outdoors.

Few studies discuss the thermal, mechanical and electrical properties of polystyrene/graphite composites [17–21], while there are some groups citing polystyrene-based conductive specimens with high EMI shielding properties [10, 14, 22–24]. However, up to now there is no record regarding the simultaneous characterization of their mechanical properties and their EMI shielding capabilities, although they should be carefully investigated simultaneously since they are both essential in any potential application.

In this work, we examine polystyrene (PS) composite films as possible candidates for EMI shielding. The PS composite films were synthesized, containing graphite as the additive, which is conductive and commercially available in large quantities for any potential commercial application. The microstructure of the as-prepared specimens as well as their electrical properties along with their electromagnetic characterization is discussed, while the mechanism of the EMI shielding effectiveness is fully analyzed. To the best of our knowledge, the present work is the first investigation of the EMI shielding and the mechanical properties of the polymer composites containing graphite filler at such high concentrations.

We provide evidence that the prepared PS-based specimens exhibit outstanding EMI shielding performance, with stiffness enhancement for graphite addition up to 40 % w/w,

while higher graphite concentration resulted in inadequate dispersion and deterioration of the mechanical performance.

2 Experimental

Polystyrene (PS) composite films were synthesized (with a thickness of ~ 200 μm), containing graphite as the additive (at concentrations ranging up to 68.31 % w/w), which is conductive and commercially available in large quantities for any potential commercial application. The composites were prepared via simple mixing of graphite powder and PS toluene solutions that were subsequently poured into absolute ethanol. Finally, after the removal of the solvent, the composites were compacted in a hot press to form polymeric films. The advantage of this approach is the ability to “freeze” the suspended graphite particles into the polystyrene matrix taking advantage of the phase inversion that takes place when the toluene solution is poured into the ethanol non-solvent.

2.1 Materials

Polystyrene (PS) pellets with a mean diameter of ~ 3 mm used in this study were obtained from Sigma-Aldrich. Graphite powder (with an average particle size < 20 μm) was also purchased from Aldrich. Anhydrous toluene and absolute ethanol (both obtained from Sigma-Aldrich) were used for the filler dispersion and the composites preparation.

2.2 Composites preparation

All the composites were synthesized by solution processing according to the following procedure. A stock solution was prepared by dissolving polystyrene pellets in toluene at various concentrations. Different amounts of graphite were dispersed in the polystyrene stock solution using ultrasonication for 20 min and vortex mixing. The solutions were, subsequently, poured into a second vial containing absolute ethanol. The aggregated products, which formed a swollen gel, were removed using tweezers, thoroughly washed with absolute ethanol and casted in glass petri dishes. The petri dishes were, then, inserted into a vacuum oven for 3 h at 70 °C to remove the remaining solvent. Finally, the composite materials were formed into thin (~ 200 μm) circular polymeric films (diameter ~ 7 cm) by compression molding using a 15T Perkin Elmer hot press at 110 °C under 3T pressure for 3 min.

2.3 Characterization

The thickness of the polystyrene/graphite composite films was measured using a digital thickness gauge, according to

UNE-ISO 4593, while their morphology was investigated using a field emission scanning electron microscopy (FE-SEM, JEOL JSM-7000F) at an acceleration voltage of 15 kV.

A TA Instruments Thermogravimetric Analyzer (SDT Q600) was used to corroborate the concentration of the graphite filler in the composites. The analysis was performed by heating ~ 10 mg of the graphite/PS composite from RT to 600 °C at a rate of 20 °C/min, under air flow. The samples were, then, held at 600 °C for 10 min before cooling.

Low-frequency impedance measurements at frequency $f = 18.33$ Hz were taken in order to obtain the electrical conductivity of the composites. Rectangular-shaped samples (sample area ~ 16 mm²) were placed between two metallic plates, forming a capacitor, as shown in Fig. 1. A reference resistor ($R_{\text{ref}} = 1$ kOhm) is connected in series with the capacitor mentioned above. Both the voltage drop, $\Delta V = V_2 - V_1$, and the phase shift, $\Delta\theta = \theta_2 - \theta_1$, are measured across the reference resistor, using a EG&G 5210 dual-phase lock-in amplifier synchronized with an AC voltage source ($V_{\text{ac}} = 2$ V), connected to the setup as shown in Fig. 1.

For the EMI characterization, a Hewlett-Packard 8722 ES vector network analyzer connected with a WR-187 rectangular waveguide was used in the frequency range 3.5–7.0 GHz, the so-called C-band of the electromagnetic spectrum, which is used for long-distance radio telecommunications, such as satellite communications transmissions, Wi-Fi devices, cordless telephones and weather radar systems. The polystyrene/graphite composite specimens were placed between the two sections of the waveguide, and the scattering parameters (S-parameters: S_{11} , S_{12} , S_{22} , S_{21}) of each sample were recorded.

Finally, the mechanical performance of the polymeric films was evaluated by means of tensile testing, using a miniature material tester with a 50 N load cell. Three to five “dog bone” tensile specimens prepared by die cutting according to ASTM 638/95 Type V international standard were clamped between the grips (30 mm initial distance) and tensioned at a crosshead speed of 0.5 mm/min according to ASTM D638. Force (in N) and deformation (in mm) were recorded during the test and converted into stress (in MPa) and strain (%), based on the cross-sectional

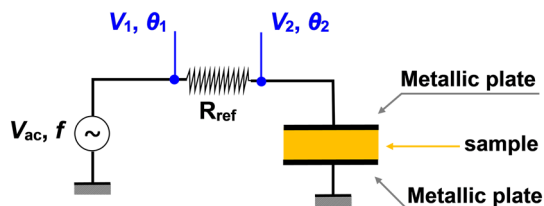


Fig. 1 Experimental setup used for the impedance measurements of the graphite/PS composites

area and the initial length data, respectively. Baseline samples (pure polystyrene, not containing graphite) were tested at the beginning of each set of samples for comparison purposes.

3 Results and discussion

3.1 Concentration of graphite filler in polystyrene polymer matrices

TGA was used in order to verify the concentration of graphite filler in the composites. Figure 2 presents the TGA curves of the graphite/PS composites from RT to 600 °C at a rate of 20 °C/min, under air flow, along with the target and the experimental % w/w concentration of graphite in the polymeric films.

As can be observed in Fig. 2, there is a slight difference between the theoretical (target) and the experimental concentration of graphite in the final composite specimens. This could be attributed to the solution processing that was used. When the toluene solution is poured into ethanol, a bad solvent for polystyrene, turbidity appears as polystyrene-poor and polystyrene-rich phases are formed. In the polystyrene-poor phases, polymer nuclei are formed by precipitation. The suspended graphite particles are entrapped inside these morphologies. The aggregates can be easily retrieved using tweezers from the solution as they form a gel-like mass. However, the yield of this technique is not 100 % efficient and there is a certain amount of polymer and filler that cannot be retrieved, resulting in the observed differences in the final concentrations.

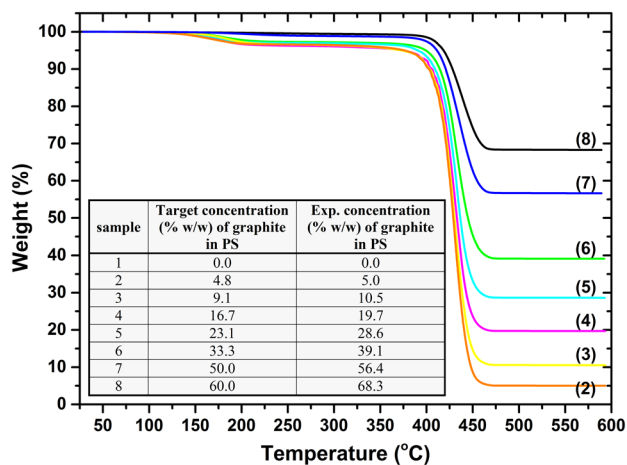


Fig. 2 TGA curves of the graphite/PS composites from RT to 600 °C at a rate of 20 °C/min, under air flow. In the inset of Fig. 1, one can see the theoretical and experimental % w/w concentration of graphite in the polymeric films

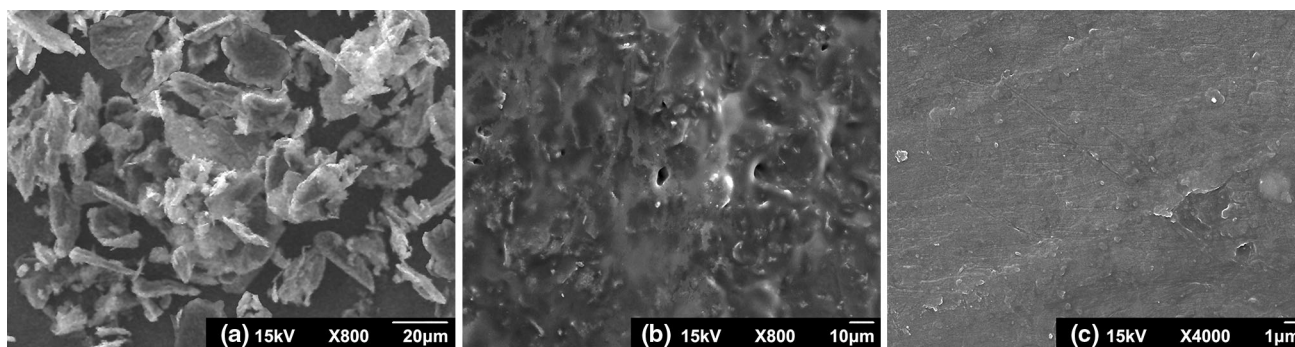


Fig. 3 SEM micrographs of pure graphite (b) and of the 39.1 % w/w polystyrene/graphite composite films before (b) and after (c) hot pressing at 110 °C under 3T pressure for 3 min, respectively

3.2 Morphology and microstructure analysis

FE-SEM was used to investigate the dispersion state of the graphite in the PS polymer matrix, along with the homogeneity of the samples. Figure 3a shows SEM micrographs of pure graphite powder, while Fig. 3b, c presents the 39.1 % w/w polystyrene/graphite composite films before and after hot pressing at 110 °C (under 3T pressure for 3 min), respectively.

As one can see from Fig. 3a, pure graphite forms microstructures with an average particle size of 20–25 μm and a thickness of almost 500 nm. Before hot pressing at 110 °C for 3 min under 3T pressure, one can notice the morphology of the graphite microstructures (see Fig. 3b), forming edges and quite rough surfaces, while the graphite filler dispersion is fairly homogeneous. After hot pressing at 110 °C, the polymeric films are smooth and good level of graphite filler dispersion can be observed, which can be mainly related to the processing method used to prepare the composite (low viscosity medium with sonication) and the selection of a proper solvent (toluene).

3.3 Electrical properties

Figure 4 depicts the electrical conductivity (σ) of the polystyrene/graphite composites as a function of the graphite concentration (% w/w). In the low concentration regime, the electrical conductivity is exceptionally low, indicating the dominating insulating character of the PS matrix. Graphite clusters, separated from each other, are distributed within the PS matrix, and thus, the charge carriers cannot move among them. However, above concentrations 20–25 % w/w, the conductivity σ increases rapidly, suggesting that this is a threshold concentration, above which graphite clusters percolate leading to conductivity enhancement; this concentration should, actually, correspond to the critical concentration c_{cr} , required for a conductive network to be formed within the polymer matrix.

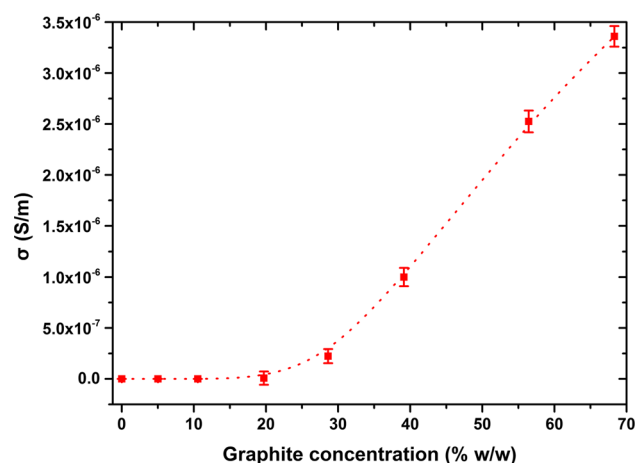


Fig. 4 Electrical conductivity (in S/m) of polystyrene/graphite composites as a function of graphite filler content. The critical concentration c_{cr} above which the film becomes conductive is 20–25 % w/w. Error bars represent the standard deviation

In the high concentration regime, conductivity increases with increasing concentration due to the fact that graphite percolation network becomes dense, allowing the charge carriers to move through multiple conductive paths. Notice that the probability of a point belonging to an infinite connected filler channel is zero below the critical concentration c_{cr} of the filler and it increases just above c_{cr} proportionally to $(c - c_{\text{cr}})^s$ with $s \approx 0.5$. However, the conductivity above the percolation threshold c_{cr} rises in a much smoother way because the first infinite conducting channels above c_{cr} are very distorted with many dead ends.

3.4 Electromagnetic interference shielding properties and mechanism

Electromagnetic shielding practically means that when an electromagnetic (EM) field is incident on a system enclosed in a shielding material, there is minimum or ideally absent transmission beyond the shielding material and into the system. Hence, the incident field is either

absorbed within the shielding material or reflected from it, as power balance dictates:

$$T + R + A = 1 \tag{1}$$

where T , R and A are the transmitted, reflected and absorbed power, respectively. A measure of the material ability to prevent the EM wave penetration is the EMI shielding effectiveness (SE). The higher the SE, the better the shielding. The SE (also denoted as SE_T , with T indicating the transmission) is usually quantified in terms of the logarithm of the incident power P_{inc} over the transmitted power P_{tm} [5, 7, 25] and thus expressed in decibels (dB) as:

$$SE = SE_T \triangleq 10 \log_{10} \left(\frac{P_{inc}}{P_{tm}} \right) = 10 \log_{10} \left(\frac{1}{T} \right) = SE_R + SE_A \tag{2}$$

where

$$SE_R = 10 \log_{10} \left(\frac{1}{1 - R} \right) \tag{3}$$

$$SE_A = 10 \log_{10} \left(\frac{1 - R}{T} \right) \tag{4}$$

SE_R and SE_A refer to the reflection and absorption SE, respectively.

Figure 5 depicts the reflection (Fig. 5a) and the absorption (Fig. 5b) spectra of the polystyrene/graphite composite films for a series of graphite concentrations, in the frequency range 3.5–7.0 GHz. Figure 5a clearly illustrates that the reflection of the polystyrene/graphite specimens is almost zero for all the graphite concentration from 0.00 to 68.3 % w/w. As a result, the EMI shielding effect

due to reflection (SE_R) is also negligible (see Fig. 5c), and in all cases, the total SE is simply $SE_T = SE_A$ [see Eq. (2)]. One can easily observe in Fig. 5d that, for graphite concentrations from 0.0 to 19.7 % w/w, the SE_A does not exceed 0.5 dB, while, for 28.6 % w/w up to 68.3 % w/w, the SE_A varies from 2.5 to 27 dB. At this point, it should be noted that a SE_T of ~15–20 dB is more than sufficient for shielding, e.g., computer devices [25], since a SE of 20 dB corresponds to the blocking of ~99 % of EM incident waves. In the present study, a SE_T of ~21–27 dB is obtained for 56.4 % w/w graphite in PS (see black curve with crosses in Fig. 5d) and a SE_T of ~24–28.8 dB for 68.3 % w/w graphite concentration in polystyrene (see red curve with ex marks in Fig. 5d), respectively, which correspond to almost 100 % blocking of the EM incident wave.

Clearly, the dominant shielding mechanism is absorption, which is also supported by the continuously increasing absorption levels with increasing graphite content in the polymeric composites. In order to gain better insight into the electromagnetic properties of the material that lead to such a particular response, we employed the retrieval method [26], modified to account for scattering data in a rectangular waveguide configuration (rather than free space as in [26]), as presented in [27]. In this method, the refractive index n and impedance z of the samples were calculated directly from the measured S-parameters S_{11} , S_{12} , S_{21} and S_{22} (note that the S-parameters S_{NM} of a NxM port network refer to the field measured at port N when port M is excited and are thus connected to the reflection and transmission of our 2 × 2 port waveguide configuration as $R = |S_{11}|^2 = |S_{22}|^2$ and $T = |S_{12}|^2 = |S_{21}|^2$). In Fig. 6, one

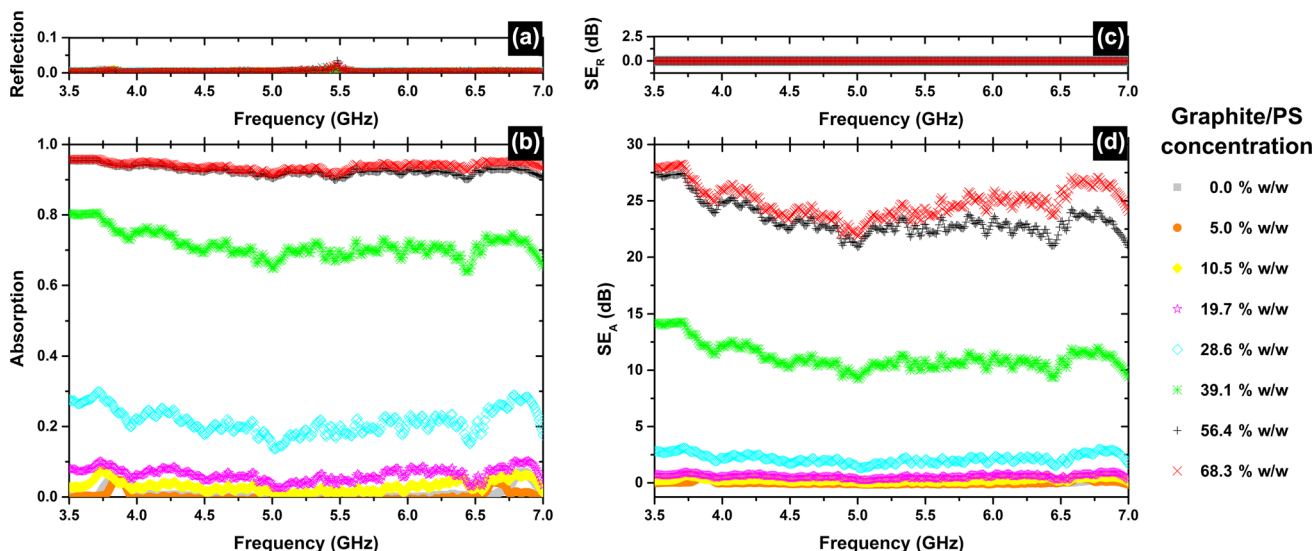


Fig. 5 Reflection (a) and absorption (b) spectra from 3.5 to 7.0 GHz (C-band) for ~200- μ m-thick polystyrene/graphite films for various filler concentrations. The electromagnetic interference shielding

effect (SE) due to reflection (SE_R ; Fig. 3c) and absorption (SE_A ; Fig. 3d) can also be seen in the frequency range 3.5–7.0 GHz

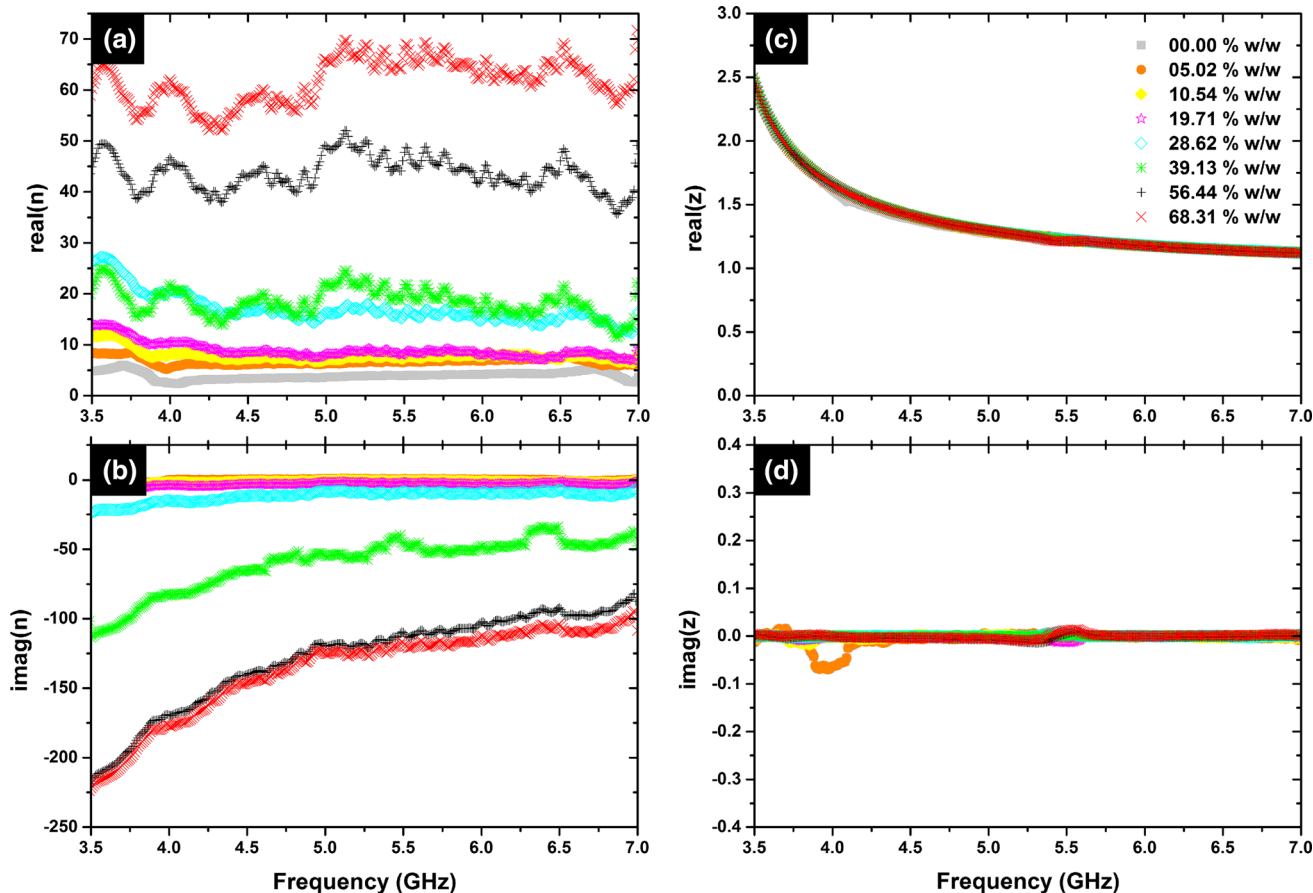


Fig. 6 Real and imaginary parts of n (a, b, respectively) and z (c, d, respectively) of polystyrene/graphite composite films, from 3.5 to 7.0 GHz

can see the real and imaginary parts of n and z for the polystyrene/graphite composite films, from 3.5 to 7.0 GHz.

The results reveal that, for concentrations below c_{cr} , the imaginary part of n is negligible as expected, but as soon as c_{cr} is reached, it starts to increase rapidly, indicating the absorption onset. The essence of the shielding mechanism though lies in the fact that the material impedance matches the free-space impedance. This impedance matching enables the incident wave to pass entirely into the material, where the high losses take over to attenuate it and prevent it from exiting. This way, not only the transmission is eliminated, but also the reflection, as has already been observed in Fig. 5a.

3.5 Mechanical properties

In order to exploit the EMI shielding capabilities of the polymer composites in practical applications, their mechanical properties should be such that they can be easily incorporated in real devices. Figure 7 illustrates the stress–strain behavior of the graphite-reinforced polystyrene films as a function of the graphite content. It should be noted that the mechanical performance of the polymeric

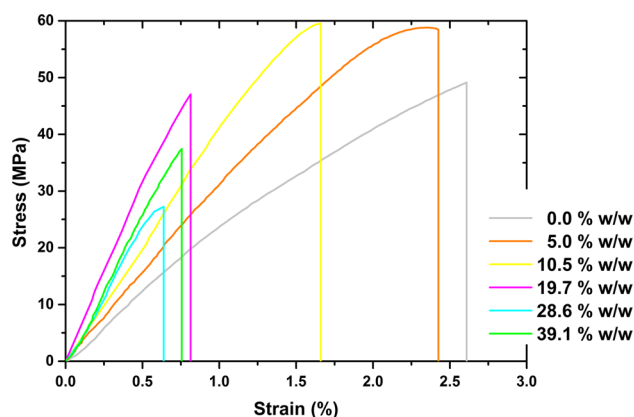


Fig. 7 Effect of graphite addition and content on the tensile response of polystyrene-based composite films

films was evaluated at least for three to five times, providing a reproducibility of 5–10 %. Moreover, it is worth mentioning that it was not possible to test films with graphite loading higher than 39.1 % w/w, due to extensive agglomeration and introduction of flaws into the polymeric films, which resulted in premature failure. Based on the slope of the linear part of the stress–strain curve, the

Table 1 Tensile strength of the PS/graphite composites under consideration, their elongation at break and Young's modulus

Sample name	Graphite concentration (%)	Tensile strength (MPa)	Elongation at break (%)	Young's modulus (GPa)
0	0	49.1	2.6	1.9
1	5	58.7	2.4	2.5
2	10.5	59.6	1.7	3.7
3	19.7	47.1	0.8	5.9
4	28.6	27.3	0.6	4.8
5	39.1	37.5	0.7	5.2

Young's modulus values of the representative specimens can be obtained. In Table 1, one can notice the tensile strength of PS/graphite composites, their elongation at break and Young's modulus, in order to evaluate the mechanical properties of these materials. Overall, the addition of graphite resulted in considerable increase in the Young's modulus of the produced polystyrene-based composite films, confirming the reinforcing role of the stiff graphite inclusions. As observed, the higher the graphite content, the higher the Young's modulus enhancement of the composite films. This holds for graphite contents up to 19.7 % w/w, which demonstrate a 230 % modulus increase compared to neat PS with 0.0 % w/w (6.3 vs. 1.9 GPa, respectively). Further, graphite addition (~28.6 and 39.1 % w/w) resulted in deterioration of the Young's modulus, which was, however, still higher than that of neat polystyrene. Moreover, graphite addition was beneficial for the tensile strength for loadings up to 10.5 % w/w, with an observed increase of ~20 %.

Compared to the stiffness, the strength improvement was limited following the addition of graphite. This can be linked with the dispersion efficiency of the graphite particles within the polystyrene matrix and the resultant morphology of the produced composites. The addition of higher amounts of graphite resulted in agglomeration phenomena, which in turn reduced the effective fiber length of the reinforcements and inhibited further improvement of the mechanical properties. It has been suggested in the past, based on the experimental data [28, 29] and micromechanical models [30] for fiber-reinforced composites, that the required fiber length to attain maximum stiffness is much lower than that required for maximum strength, making stiffness less sensitive to the critical fiber length and fiber orientation/distribution compared to strength. Overall, it can be concluded that films with 39.1 % w/w graphite content are good candidates for practical applications, since they show higher stiffness compared to neat PS, adequate strength (>35 MPa) as well as efficient EMI shielding (absorbance ~80 %; SE = 10–15 dB).

4 Summary

Polystyrene composite films were fabricated (with a thickness of ~200 μm), containing graphite at concentrations up to ~70 % w/w. Their electromagnetic properties were investigated in the so-called C-band of the electromagnetic spectrum (3.5–7.0 GHz), which is typically used for long-distance radio telecommunications; the mechanism of their electromagnetic shielding effectiveness is fully analyzed. It is demonstrated that the prepared polymer composite films exhibit outstanding electromagnetic shielding performance, which makes them potential candidates for several electronics applications. Moreover, the mechanical properties of the prepared polymeric films were carefully studied, which are essential in real-world applications. Samples with 39.1 % w/w graphite content are good candidates for practical applications, since they show higher stiffness compared to plain polystyrene and adequate strength (>35 MPa) in conjunction with efficient EMI shielding (absorbance ~80 %; SE = 10–15 dB). To the best of our knowledge, the present study probes for the first time the electromagnetic shielding efficiency and the mechanical properties of the polymer composite film specimens containing graphite as a filler at such high concentrations.

Acknowledgments This work was supported by the European Research Council under ERC Advanced Grant No. 320081 (PHOTOMETA). Work at Ames Laboratory was partially supported by the Department of Energy (Basic Energy Sciences, Division of Materials Sciences and Engineering) under Contract No. DE-AC02-07CH11358. Financial support by the EU-FET Graphene Flagship (Grant Agreement No: 604391) is also acknowledged. Author Z.V. acknowledges the FP7-REGPOT 2012-2013 (Grand Agreement No 316165). The authors also acknowledge Dr. S. Droulias for the employment of the retrieval method calculating the refractive index n and impedance ζ of the samples and for his useful comments on the manuscript.

References

1. X.C. Tong, *Advanced Materials and Design for Electromagnetic Interference Shielding* (Taylor & Francis Group, London, 2009)
2. S. Geetha, K.K.S. Kumar, C.R.K. Rao, M. Vijayan, D.C. Trivedi, *J. Appl. Polym. Sci.* **112**, 2073–2086 (2009)
3. S. Celozzi, R. Araneo, G. Lova, *Electromagnetic Shielding* (Wiley, New York, 2008)
4. M. Sucheai, I.V. Tudose, G. Tzagkarakis, G. Kenanakis, M. Katharakis, E. Drakakis, E. Koudoumas, *Appl. Surf. Sci.* **352**, 151–154 (2015)
5. A. Ameli, P.U. Jung, C.B. Park, *Carbon* **60**, 379–391 (2013)
6. J.-M. Thomassin, C. Jerome, T. Pardoën, C. Bailly, I. Huynen, C. Detrembleur, *Mat. Sci. Eng. R* **74**, 211–232 (2013)
7. M.H. Al-Saleh, W.H. Saadeh, U. Sundararaj, *Carbon* **60**, 146–156 (2013)
8. B. Hornbostel, P. Potschke, D. Kornfeld, J. Kotz, S.J. Roth, *Nanostruct. Polym. Nanocompos.* **3**, 103–107 (2007)

9. P.C.P. Watts, W.K. Hsu, H.W. Kroto, D.R.M. Walton, *Nano Lett.* **3**, 549–553 (2003)
10. Y.L. Yang, M.C. Gupta, K.L. Dudley, R.W. Lawrence, *Nano Lett.* **5**, 2131–2134 (2005)
11. S.K. Hong, K.Y. Kim, T.Y. Kim, J.H. Kim, S.W. Park, J.H. Kim, B.J. Cho, *Nanotechnology* **23**, 455704 (2012)
12. H.M. Kim, K. Kim, C.Y. Lee, J. Joo, S.J. Cho, H.S. Yoon, D.A. Pejaković, J.W. Yoo, A.J. Epstein, *Appl. Phys. Lett.* **84**, 589 (2004)
13. M.J. O’Connell, *Carbon Nanotubes: Properties and Applications* (Taylor and Francis, London, 2006)
14. G.A. Gelves, M.H. Al-Saleh, U. Sundararaj, *J. Mater. Chem.* **21**, 829–836 (2010)
15. V. Panwar, J.-O. Park, S.-H. Park, S. Kumar, R.M. Mehra, *J. Appl. Polym. Sci.* **115**, 1306–1314 (2010)
16. T. Kuilla, S. Bhadra, D. Yao, N.H. Kim, S. Bose, J.H. Le, *Prog. Polym. Sci.* **35**, 1350–1375 (2010)
17. M. Fang, K. Wang, H. Lu, Y. Yang, S. Nutt, *J. Mater. Chem.* **19**, 7098–7105 (2009)
18. F.M. Uhl, C.A. Wilkie, *Polym. Degrad. Stab.* **76**, 111–122 (2002)
19. R.K. Goyal, P.A. Jagadale, U.P. Mulik, *J. Appl. Polym. Sci.* **111**, 2071–2077 (2009)
20. R. Sengupta, M. Bhattacharya, S. Bandyopadhyay, A.K. Bhowmick, *Prog. Polym. Sci.* **36**, 638–670 (2001)
21. W.-P. Wang, C.-Y. Pan, *Polymer* **45**, 3987–3995 (2004)
22. D.-X. Yan, P.-G. Ren, H. Pang, Q. Fu, M.-B. Yang, Z.-M. Li, *J. Mater. Chem.* **22**, 18772–18774 (2012)
23. S. Maiti, N.K. Shrivastava, S. Suin, B.B. Khatua, *ACS Appl. Mater. Interfaces* **12**, 4712–4724 (2013)
24. G.A. Gelves, B. Lin, U. Sundararaj, J.A. Haber, *Adv. Funct. Mater.* **16**, 2423–2430 (2006)
25. M.H. Al-Saleh, G.A. Gelves, U. Sundararaj, *Comp. Part A* **42**, 92–97 (2011)
26. D.R. Smith, S. Schultz, P. Markos, C.M. Soukoulis, *Phys. Rev. B* **65**, 195104 (2002)
27. H. Chen, J. Zhang, Y. Bai, Y. Luo, L. Ran, Q. Jiang, J. Au Kong, *Opt. Express* **14**, 12944–12949 (2006)
28. J.L. Thomason, M.A. Vlug, *Compos. A* **27A**, 477–484 (1996)
29. J.L. Thomason, M.A. Vlug, G. Schipper, H.G.L.T. Krikor, *Compos. A* **27A**, 1075–1084 (1996)
30. A. Kelly, W.R. Tyson, *J. Mech. Phys. Solids* **13**, 329–350 (1965)